RIGA TECHNICAL UNIVERSITY

Faculty of Mechanical Engineering, Transport and Aeronautics
Institute of Mechanics and Mechanical Engineering

Sergejs Ločs

Doctoral Student of the Study Programme "Production Technology"

LASER CLADDED SURFACE HARDENING COATING WITH GRADIENT OF MECHANICAL PROPERTIES

Summary of the Doctoral Thesis

Scientific supervisor
Professor Dr. sc. ing.
IRĪNA BOIKO

RTU Press
Riga 2020

DOCTORAL THESIS PROPOSED TO RIGA TECHNICAL UNIVERSITY FOR THE PROMOTION TO THE SCIENTIFIC DEGREE OF DOCTOR OF SCIENCE

To be granted the scientific degree of Doctor of Science (Ph. D.), the present Doctoral Thesis has been submitted for the defence at the open meeting of RTU Promotion Council on July 15, 2020 at ………. at the Faculty of Mechanical Engineering, Transport and Aeronautics of Riga Technical University, 6B Kipsalas Street, Room 402.

OFFICIAL REVIEWERS

Professor Dr. sc. ing. Ēriks Geriņš
Riga Technical University, Latvia

Professor Dr. sc. (Doctor of Technical Science) Alexander S. Kalinichenko
Belarusian State Technological University, Belarus

First Deputy Director Ph. D. Vadim V. Savich
State Scientific Institution "Powder Metallurgy Institute", Belarus

DECLARATION OF ACADEMIC INTEGRITY

I hereby declare that the Doctoral Thesis submitted for the review to Riga Technical University for the promotion to the scientific degree of Doctor of Science (Ph. D.) is my own. I confirm that this Doctoral Thesis had not been submitted to any other university for the promotion to a scientific degree.

Sergejs Ločs ……………………………. (signature)
Date: ………………………

The Doctoral Thesis has been written in Latvian. It consists of an Introduction; 6 Chapters; Conclusions; 130 figures; 37 tables; 14 appendices; the total number of pages is 175. The Bibliography contains 163 titles.

CONTENTS

GENERAL CHARACTERISTICS OF THE THESIS

Actuality of the topic

Damages to machine components and tools during operation mainly occur due to surface collapsing processes. Therefore, coating technology is currently receiving a lot of attention in the metalworking workforce, especially in the fields of aerospace, mechanical engineering, shipbuilding, tooling, etc. As a result, the global shortage of materials and energy resources is leading to the introduction of innovative technologies and materials to extend product life at maximum performance levels in balance with economic efficiency and with less impact on the environment.

Laser cladding is an advanced coating technology that is widely used to improve the physicomechanical and tribotechnical properties of surfaces on metallic components. Due to its advantages over thermal spraying and welding processes, this process is widely used for hardfacing, refurbishment and repairing of high value machine parts and tools (turbine blades, engine components, injection molding tools, etc.) [1]–[4]. Also, additive manufacturing (AM), which involves the fabrication of sophisticated forms of 3D details in layers according to the geometry of a computer-aided design (CAD) model, has been successfully applied in laser cladding [5]–[7].

On the other hand, there are still problems with the cladding of tool steels and composite materials, which create coatings and additive manufacturing technology 3D objects that are designed to work in harsh working conditions. Typical defects are cracking and detachment, which occur both during product life and directly during the technological process [8]–[15]. The reasons are the effects of high temperature and the physicomechanical properties of these materials that differ from those of the base material, resulting in high residual stresses on the coating and substrate interface, which significantly degrade the quality and performance of the coatings [1], [16].

One of the most promising directions for solving these problems is the development of functionally graded coatings. Coatings of this type exhibit heterogeneity of properties in the direction normal to the volume of material, which allows the properties of the coating and base material to be approximated to achieve the required combination of toughness and adhesion strength. Gradient coatings are applied to advanced grade materials. The gradient of properties in the material is induced by changes in chemical composition, physical structure, and mechanical properties [16].

Thus, the development of a laser cladding method for obtaining surface hardening coatings with a gradient of mechanical properties for hardening and refurbishing surfaces of machine elements and tools is a topical scientific-technical task.

Aim and Objectives of the Thesis

The aim of the Thesis is to research the possibility of creating a laser cladded single layer surface hardening coating with a gradient of mechanical properties in the direction normal from the surface to the base material to increase the crack resistance of coatings and

consequently extend the workability of products in manufacturing and refurbishment of machine elements and tools.

The following objectives were set to achieve the aim.

1. Research on the significance of coatings, theoretical analysis of laser cladding technology, and study of the current situation; determination of essential technological parameters of laser cladding process and coating quality characteristics.

2. Experimental research of the influence of technological parameters of the laser cladding process (cladding speed and laser beam defocusing) on the quality characteristics (shape geometry parameters, the amount of carbide-forming elements in the clad layer, and porosity) of a single pass high-speed steel clad with keyhole in penetration.

3. Experimental research of the conditions for the formation of qualitative characteristics (thickness, depth of the penetration, amount of carbide forming elements in the cladding layer, character of the microhardness change in the coating-substrate system, defects) of high-speed steel coatings with keyhole in penetration depending on laser cladding regimes. Evaluate the effect of post cladding heat-treatment (annealing) on the properties of coatings.

4. Experimental research of the influence of coating's anisotropic structure on surface properties of laser cladded high-speed steel coatings after machining process, and study of the effects of technological parameters (cladding speed, overlap ratio of single clad beads, laser beam focus offset) on the quality and functional properties of coatings (coating thickness, coating surface hardness and friction coefficient).

5. Performing a comparative analysis of high-speed steel coatings produced by different laser cladding methods.

Research Methods

To achieve the aim of the Doctoral Thesis and its tasks, practical research methods, statistical processing of experimental results, analytical, comparative and graphical methods were used; metallographic studies of coatings, examination of hardness and microhardness, surface roughness and tribotechnical properties were carried out; optical and scanning electron microscopy (SEM) as well as energy dispersive X-ray spectrometry (EDS) analysis was performed. The following computer software was used to perform the tasks and graphically represent the results: *Mastercam, Robotmaster, Minitab, Microsoft Office, InstrumX, VegaTC, INCA Energy* and *OriginPro.*

Scientific Novelty

For the first time, the regularities of laser cladded coatings with keyhole in penetration were studied, and, based on this research, a new laser cladding method, which allows obtaining a single layer surface hardening coating with a gradient of mechanical properties using one component additive material, was proposed.

Using the newly introduced laser cladding method, a detailed study of the effect of laser cladding process regimes on the quality characteristics forming the conditions of single bead

laser clads and coatings using a high-speed steel (AISI M2) filler material was carried out, and based on this study the following was found out:

- o Areas of laser cladding process regime (laser irradiance maximum power density of $4.87 \cdot 10^3$–$7.73 \cdot 10^3$ W/mm^2, cladding speed of 600–1500 mm/min), which provides forming of cladded layer with keyhole in penetration, thus creating a coating with a gradient of mechanical properties in the coating-substrate system, were detected.
- o Empirical models of geometric characteristics, amount of carbide-forming elements and hardness of laser cladded coating with keyhole in penetration in terms of the basic process parameters were obtained, which enable to have control over the quality characteristics and properties of the coatings to be formed.
- o In the study of geometric characteristics of coatings, characterization of microhardness change from surface to substrate and crack formation, it was determined that laser cladding of non-cracked coatings can be achieved within the microhardness gradient range of 107–295 HV/mm, without the use of heat treatment.
- o As a result of study of comparative properties of laser cladded coatings with and without keyhole in penetration, it was determined that the laser cladding with keyhole in penetration allowed a significant reduction of the gradient of mechanical properties (6.8 times) in the transition zone between the coating and base material comparing to the laser cladding process with minimal penetration while maintaining a high level of tribotechnical properties.

Practical Significance of the Thesis

1. The results of research on the conditions of formation of single bead laser clads and coatings can be used to improve the technology of laser cladding of functional coatings and additive manufacturing as well, to manufacture and refurbish machine elements and tools.
2. The obtained laser cladding method may exclude deposition of the buffer layers on the substrate in processes of cladding of dissimilar steels and additive manufacturing of 3D objects, which contribute to the improvement of the mechanical properties of the base material near-surface layers of products operating under cyclic load with variable signs and thermocyclic conditions.
3. Technological recommendations for the application of the new laser cladding method for hardfacing and refurbishment of pressure shaping tools are given.
4. Using the new laser cladding method, the parts of the pressure shaping equipment in practice were refurbished in praxis: Santroplasts Ltd. (Latvia), Research Laboratory for Processing Materials BNTU (Belarus), which was approved by the company test acts (Annexes 1 and 2).

Practical Application

With this method, a wide range of alloyed steels can be laser cladded to produce high-quality surface hardening coatings and can be used in the manufacture and refurbishment of both pressure shaping equipment and machine components that can operate under cyclic

mechanical loads at hard working conditions, to improve properties (fatigue and wear resistance) of component work surfaces.

Besides, it is possible to manufacture parts from low-grade non-alloy steels with subsequent laser cladding of alloy steels on work surfaces, which significantly increases the hardness and abrading resistance of the coated substrate and reduces consumption of extremely deficient materials.

The Author of the Thesis defends

1. Laser cladding method, which allows obtaining the surface hardening coating with a gradient of mechanical properties in the coating-substrate system.
2. Results of experimental research of the influence of technological parameters of the laser cladding process (cladding speed and laser beam defocusing) on the quality characteristics (geometry, amount of carbide-forming elements in the clad, and porosity) of a single bead high-speed steel clad with keyhole penetration, which allowed to determine the best combination of technological parameters.
3. Results of experimental research of technological parameters (cladding speed, overlap ratio, powder mass feed rate) influence on the high-speed steel coating quality characteristics (thickness, depth of the penetration, amount of carbide forming elements in the cladding, hardness, and friction coefficient), which allowed to determine the best laser cladding regimes.
4. Evaluation of the influence of technological parameters (cladding speed, laser beam defocusing, powder mass feed rate, overlap ratio of single beads) on the quality characteristics of coatings (geometric parameters, amount of carbide-forming elements, hardness and friction coefficient).

Approbation of Obtained Results

The main results of the Doctoral Thesis were published in peer-reviewed scientific publications, as well as reported and discussed at local and international conferences.

Conference Reports

1. Ločs, S. "Vienslāņa virsmas nocietinošo pārklājumu ar mehānisko īpašību gradientu lāzeruzkausēšanas metode". Rīgas Tehniskās universitātes 60. starptautiskā zinātniskā konference, Transporta, mašīnzinību un aeronautikas fakultātes sekcija "Ražošanas tehnoloģija", 2019. g., 14. oktobris, Rīga, Latvija.
2. Ločs, S. "High speed steel functionally graded coating by laser cladding". International practical conference at Šiauliai University "Towards Smart Industry in Lithuanian and Latvian Regions: Opportunities and Challenges", 18 April 2019, Šiauliai, Lithuania.
3. Ločs, S. "Ātrgriezējtērauda pārklājumu ar funkcionālu gradienta struktūru lāzera uzkausēšana". Rīgas Tehniskās universitātes 59. starptautiskā zinātniskā konference, Transporta un mašīnzinību fakultātes sekcija "Ražošanas tehnoloģija", 2018. g., 11. oktobris, Rīga, Latvija.

4. Locs, S., Leitans, A., Tamanis, E., Drozdovs, P., Dovoreckis, J., Devoino, O. "HSS Coating with Keyholes in Penetration Produced by Laser Cladding Process". 9th International Conference „Beam Technologies & Laser Application", 17–19 September 2018, Saint-Petersburg, Russia.

5. Locs, S., Boiko, I. "Quality assessment of laser cladded HSS coatings with deep penetration into base material to obtain a smooth gradient of properties in coating-substrate interface". 9th International Conference „Biosystems Engineering 2018", 9–11 May 2018, Tartu, Estonia.

6. Ločs, S., Boiko, I. "Lāzera uzkausēšanas režīmu ietekme ātrgriezējtērauda AISI M2 pārklājumu kvalitāti un mehāniskajām īpašībām". Rīgas Tehniskās universitātes 58. starptautiskā zinātniskā konference, Transporta un mašīnzinību fakultātes sekcijas "Inženiertehnika, mehānika un mašīnbūve", apakšsekcija "Ražošanas tehnoloģija", 2017. g., 12. oktobris, Rīga, Latvija.

7. Locs, S., Boiko, I., Drozdovs, P., Dovoreckis, J., Devoyno, O. "Investigation of Coaxial Laser Cladding Process Parameters Influence onto Single Pass Clad Geometry of Tool Steel". 8th International Conference "Biosystems Engineering 2017", 11–12 May 2017, Tartu, Estonia.

8. Ločs, S., Boiko, I. "Lāzera uzsmidzināšanas tehnoloģiju izpēte". Rīgas Tehniskās universitātes 57. starptautiskā zinātniskā konference, Transporta un mašīnzinību fakultātes sekcijas "Inženiertehnika, mehānika un mašīnbūve", apakšsekcija "Ražošanas tehnoloģija", 2016. g., 18. oktobris, Rīga, Latvija.

9. Locs, S., Boiko I. "Research of Laser Cladding of the Powder Materials for Die Repair", 25th International Baltic Conference of Engineering Materials & Tribology "BALTMATTRIB 2016", 3–4 November 2016, Riga, Latvija.

Publications

1. **Ločs, S.**, Leitāns, A., Tamanis, E., Drozdovs, P., Dovoreckis, J., Devoino, O. HSS Coating with Keyholes in Penetration Produced by Laser Cladding Process. Journal of Physics: Conference Series, 2018, Vol.1109, pp. 1–10. ISSN 1742-6588. e-ISSN 1742-6596. Available from: doi:10.1088/1742-6596/1109/1/012063. (SCOPUS, IOPscience)

2. **Ločs, S.**, Boiko, I. Quality Assessment of Laser Cladded HSS Coatings with Deep Penetration into Base Material to Obtain a Smooth Gradient of Properties in Coating-Substrate Interface. Agronomy Research, 2018, Vol.16, Special Iss.1, pp. 1095–1109. ISSN 1406-894X. Available from: doi:10.15159/AR.18.094. (SCOPUS)

3. **Ločs, S.**, Boiko, I., Leitāns, A., Drozdovs, P. Experimental Study of Coaxial Laser Cladding of Tool Steel. In: 16th International Scientific Conference "Engineering for Rural Development": Proceedings. Vol. 16, Latvia, Jelgava, 24–26 May, 2017. Jelgava: 2017, pp. 1038-1046. ISSN 1691-5976. Available from: doi:10.22616/ERDev2017.16.N219. (SCOPUS, ISI Web of Science)

4. Bulaha, N., **Ločs, S**. Research in Surface Roughness for Laser Cladding Coatings. In: 16th International Scientific Conference "Engineering for Rural Development": Proceedings. Vol. 16, Latvia, Jelgava, 24–26 May, 2017. Jelgava: 2017, pp. 1131-1138. (SCOPUS, ISI Web of Science)

5. **Ločs, S.**, Boiko, I., Drozdovs, P., Dovoreckis, J., Devoyno, O. Investigation of Coaxial Laser Cladding Process Parameters Influence onto Single Pass Clad Geometry of Tool Steel. Agronomy Research, 2017, Vol. 15, pp. 1–15. ISSN 1406-894X. Available from: doi:10.15159/AR.17.018 (SCOPUS)

6. Boiko, I., **Ločs, S.**, Devoino, O., Drozdovs, P. Investigation of Coaxial Laser Cladding of Tool Steel. In: Proceedings of 10th International Simposium "Powder Metallurgy. Surface Engineering, New Composite Materials, Welding", Belarus, Minsk, 5–7 April 2017. Minsk: Belarusskaya Navuka, 2017, pp. 92–101. ISBN 978-985-08-2131-7. (in Russian)

7. **Ločs, S.**, Boiko, I., Mironovs, V., Tamanis, E., Devoyno, O. Research of Laser Cladding of the Powder Materials for Die Repair. Key Engineering Materials, 2017, Vol. 721, pp. 280–284. ISSN 1662-9795. Available from: doi:10.4028/www.scientific.net/KEM.721.280. (SCOPUS)

Structure and Content of the Thesis

The Thesis is written in Latvian, it contains an introduction, 6 chapters, conclusions, bibliography, 14 appendixes, 130 pictures, 37 tables, and 175 pages in total, not including appendixes. 163 sources of information were used.

BRIEF DESCRIPTION OF THE THESIS

In the Introduction the topicality of the Doctoral Thesis is justified, the aim of the research is stated and justified, and the tasks of the Thesis are defined.

1. Literature Review

This section reviews the literature on the role of metallic coatings and the processes used to create them. The scientific-technical level analysis of laser cladding technology was carried out, which allowed obtaining information about the peculiarities, applicability, inherent advantages and disadvantages of this process. Difficulties in tool steel cladding were found to be due to the highly concentrated energy of laser radiation resulting in a rigid thermal regime in the superficial layers due to high heating and cooling rates. Thus, a sharp thermal gradient coupled with a high solidification rate in the melting zone causes formation of solid and brittle phases, as well as the magnitude of residual stresses, which results in an increased risk of cracking [11], [17]–[20].

In addition, an analysis of the current cladding technologies has shown that formation of unfavourable tensile stresses in the top layers results in reduction in the fatigue strength of the refurbished parts. Due to such a significant disadvantage, the use of cladding technologies is often one of the stopping causes, as cyclic loading can lead to premature distortion and breakdown of the part [21]–[24].

As a result of the literature review, the quality characteristics and parameters of the coatings, as well as the factors that influence them, were determined. When reviewing research reports, it was noted that the main task of several works is mainly to minimize dilution of the coating by the substrate, since excessive mixing with the base material is considered to adversely affect the mechanical properties of the coating. In turn, traditional monolithic coatings with minimal depth of penetration are often unable to withstand extreme operating conditions because they are primarily due to the drastic change in physicomechanical properties of the coating and substrate transition area, which induces a high level of residual stress concentration at the interface, which results in a distortion of the surface. As a result, research and various attempts to create functionally gradient coatings are underway [16], [25]. However, certain methods of forming this type of coating significantly increase duration of the technological process, and in most cases do not eliminate the fundamental problem of excluding the sharp transition of properties in the bonding zone between the coating and the base material.

In general, the analysis of the scientific literature shows that the laser cladding process has not yet been researched sufficiently, as this technology is constantly evolving: new types of lasers and new materials occur, equipment is being modernized. In addition, the complexity of process research is determined by the large number of influencing factors, each of which makes a significant contribution to the change in coating properties.

Therefore, there is still an industrial need for obtaining of a more appropriate cladding technology for hardening and refurbishment of part contact surfaces, as well as for creating spatial structures that allow for high quality coatings and 3D objects with increased performance while maintaining product performance over the intended operating period.

2. Methodology and Means of Experimental Studies

This section provides information on methods, equipment and materials used in experimental research. Experimental work was carried out using a robotic laser processing complex (Fig. 2.1 a), which allows performing of a coating by laser cladding. In all experimental studies, a spherical shape high-speed steel AISI M2[1] metal powder of 53–150 μm granulometric composition was used for cladding coatings and single beads.

High-speed steel provides high strength, hardness, and wear resistance. Along with its applicability in cutting tools, this class of steels is also used in stamping tools, which can be used in extremely harsh conditions – pressures above 2000 MPa, temperature of 300–500 °C and even higher, in large-scale and mass production, when it is necessary to ensure high durability of stamping equipment [26].

Experimental cladding in this research was performed on medium, high carbon and alloy steel substrates (DIN 66Mn4[2], EN 41Cr4[3], EN C80U[4], AISI D2[5]). The experimental specimens were pre-grinded, with overall dimensions of 100 mm × 100 mm × 10 mm.
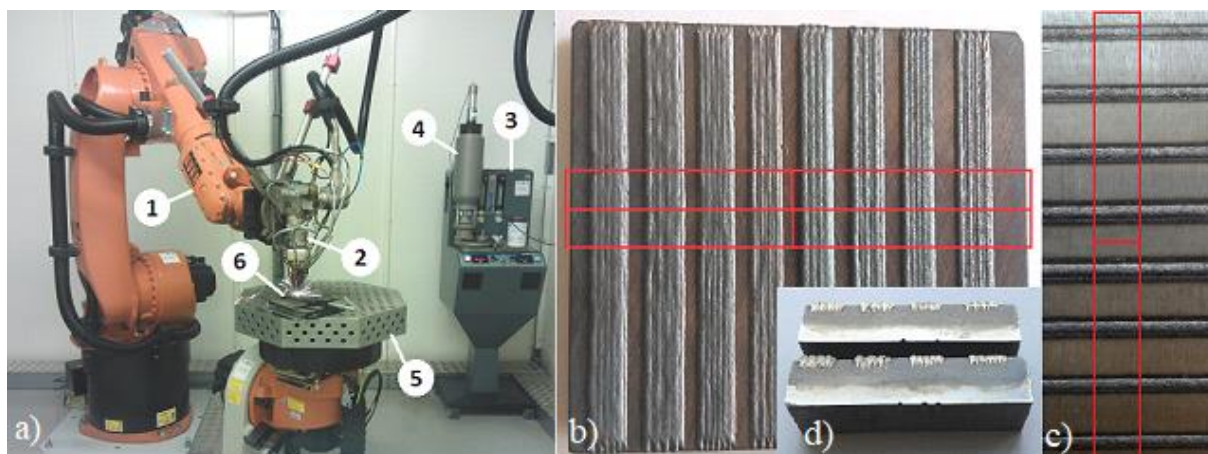

Fig. 2.1. Laser cladding equipment (a); location of cross-sections for microspecimens producing (b); a series of single bead clads (c); etched (Nital 4 %) microspecimens (d).
1 – six-axis industrial robot manipulator; 2 – laser cladding tool; 3 – metal powder feeder;
4 – metal powder loading chamber; 5 – two-axis rotary positioner; 6 – sample processed.

---

[1] Molybdenum-tungsten high-speed steel, specified by the AISI designation system (ASTM A600-92a), according to the material quality certificate. Equivalent European mark designation: HS6-5-2 (LVS EN ISO 4957:2001).

[2] Alloy structural steel, designation according to quality certificate: 65G (GOST 14959-79). The text refers to the equivalent European mark designation in the DIN system [27].

[3] Alloy structural steel, designation of quality certificate: 40H (GOST 4543-71) The text refers to the equivalent European mark designation (LVS EN 10083-3:2006).

[4] Non-alloy tool steel, quality certificate designation: U8 (GOST 1439-99). The text refers to the equivalent European mark (LVS EN ISO 4957: 2001).

[5] Alloy tool steel, designated by the AISI standard designation system (ASTM A681-08). The text refers to the equivalent European mark: X153CrMoV12 (LVS EN ISO 4957:2001).

To implement the tasks of the present Doctoral Thesis, the research was focused on the metallographic study of laser cladded beads and coatings, performed on microspecimens of samples cross-sections (Fig. 2.1 b–d).

In order to obtain predictive indices of the quality characteristics of coatings, the main tasks of this study were to determine the regularities of the influence of technological parameters of laser cladding process on the quality characteristics of coatings (geometric parameters of coatings and single bead clads, hardness, amount of carbide-forming elements in the cladded layer, coefficient of friction and porosity).

For this purpose, research of the relationship between technological parameters and coating quality characteristics was performed by using multifactorial experimental design methods and regression analysis. As a result, empirical regression models for prediction of coating quality characteristics, expressed as a first-order polynomial (Eq. (2.1)), were obtained [28], [29]:

$$\hat{y} = b_0 + \sum_{i=1}^{n} b_i x_i, \tag{2.1}$$

where

$\hat{y}$ – the response variable calculated by the regression model;

x_i – factor or parameter of the process;

b_0, b_i – regression coefficients;

i – index of values of actual variables;

n – number of variables.

The statistical significance of the regression-based empirical prediction models and their factors was estimated by analysis of variance ANOVA (*Analysis of Variance*), using the *Minitab* application. This method allows estimating the adequacy of the regression model by performing a null hypothesis test using Fisher's *F*-criterion at the given level of significance ($\alpha \leq 0.05$).

A coefficient of determination (R^2) was used to evaluate the quality of the obtained models, which shows what part of the total scattering of the response is explained by changes in the regressors. The closer the coefficient value is to 1 or 100 %, the closer the output parameter is to the factors [30]–[33]. For acceptable models, the coefficient of determination shall be not less than 50 %, in which case the value of the correlation coefficient (r_{xy}) shall be greater than 70 %.

The mathematical accuracy test of the regression models was carried out by calculating the average relative approximation error by equation (2.2) [34], also called the mean absolute percentage error [29].

$$\bar{A}_\varepsilon = \frac{1}{n} \sum_{i=1}^{n} \left| \frac{y_i - \hat{y}_i}{y_i} \right| \cdot 100, \ \%, \tag{2.2}$$

where

n – sample size;

y_i – experimental values of the response;

$\hat{y}_i$ – values of the response, calculated from the regression equation.

3. Study of Quality Characteristics of Laser Cladded Single Bead With Keyholes in Penetration

In this chapter, the influence of process parameters (cladding speed V, mm/min and laser beam defocusing F_Z, mm) on the quality characteristics of the single clad bead with a keyhole in penetration: shape geometry parameters (Fig. 3.1), porosity and amount of carbide-forming elements in a clad were analyzed.
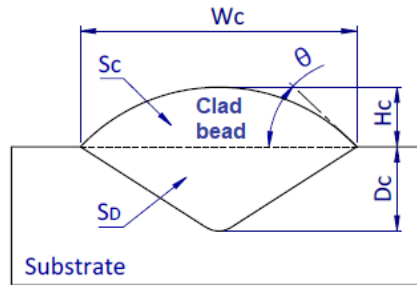

Fig. 3.1. Schematic representation of the single bead clad, and shape designation: H_C – height of the bead; W_C – width of the bead; θ – contact angle; D_C – depth of the penetration; S_C – area of the bead; S_D – area of the penetration.

Experimental Materials, Settings, Planning and Evaluation methods

The experimental beads were cladded onto spring steel sheets (DIN 66Mn4). To investigate the interaction of all variables, the Taguchi[1] experiment planning method was chosen, which resulted in experiment planning matrices (Taguchi orthogonal arrays) L_{16} (4^2) [34] for the two defocusing directions respectively, one of them being a negative F_{Z1}: (–3...0) and the other one a positive F_{Z2}: (+3...0) direction. Experimental factors and variation levels for each defocusing direction are summarized in Table 3.1.

Table 3.1

Factor Levels and Variation Intervals in Respect to the Defocusing Direction

Negative defocusing				
Factors	Levels			
V – cladding speed, mm/min	1500	1200	900	600
F_{Z1} – focus shift, mm	–3	–2	–1	0
Positive defocusing				
Factors	Levels			
V – cladding speed, mm/min	1500	1200	900	600
F_{Z2} – focus shift, mm	+3	+2	+1	0

Other technological parameters were set as constant values during laser cladding process: laser output power 1000 W, shielding gas (Ar) flow 15–16 L/min, powder carrier gas (Ar) flow 5 L/min, powder mass feed rate 7 g/min, nozzle stand-off distance 8 mm, preheating temperature of base materials 100 °C.

---

[1] Statistical method of planning by Genichi Taguchi.

In the course of the research, the relation between the quality characteristics of laser cladded single beads and the technological parameters of the process was considered and summarized in diagrams. In addition, regression analysis resulted in empirical models, which are characterized by the following response function:

$$Y_i = f(F_Z, V), \qquad (3.1)$$

where the following criteria were adopted for the response variables or optimization parameters Y_i: H_C − height of the cladded bead, mm; W_C − width of single bead clad, mm; D_C − depth of penetration, mm; θ − contact angle, °; P_C − porosity, %; E_C − amount of carbide-forming alloying elements (Cr, Mo, W, V) in the clad, wt. %.

The porosity value was expressed in percentage by calculating the relative area of porosity in the cross-section, i.e. ratio of pore areas to the total bead area. The amount of alloying elements was determined by EDS analysis for each bead, marking the area of the zone to be analysed in the cladded layer by software (Fig. 3.2).
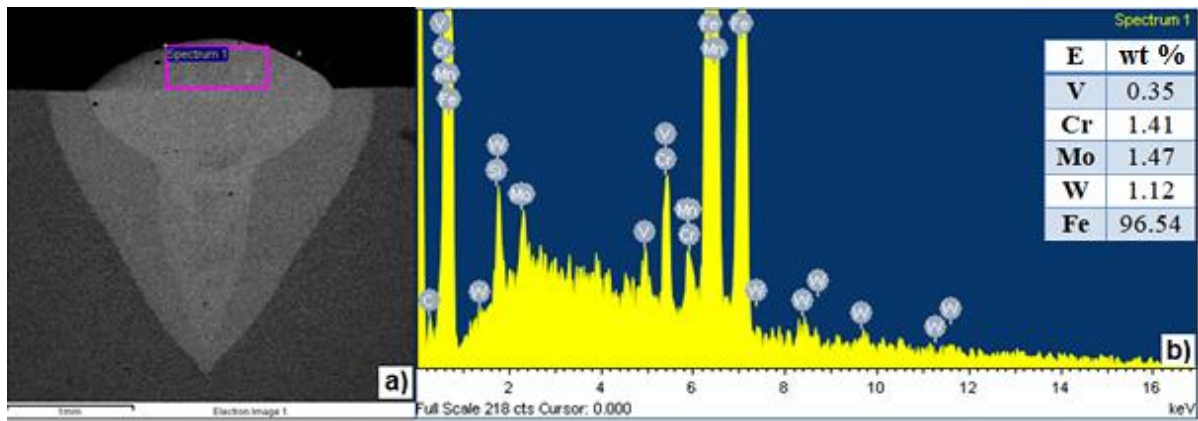

Fig 3.2. EDS Analysis of cladded bead: SEM image of single bead clad cross-section (a); characteristic X-ray spectra of the chemical elements identified in the demarcated area (b).

Main Results and Conclusions of the Experiment

The following characteristic zones are marked in the cross-section of the cladded bead (Fig. 3.3 a): the clad zone, which is the area above the base surface (CZ), the keyhole penetration zone (KPZ) and the heat affected zone (HAZ). In the cross-sectional examination of beads, it was noted that some beads contain gas pore inclusions, which were arranged randomly but mostly along the central axis of the bead. In laser welding, this phenomenon is associated with a high laser beam power density in the focal spot because, impacting the material in this mode, the molten metal part in the melt pool transits into a vapor state which causes gas bubbles to appear. Thus, due to the rapid solidification of the melt pool, the pores remain enclosed in the subsurface layer [36]–[39]. Measured pore diameters range from 50 μm to 300 μm. The measured geometric parameters of the shape are shown in Fig. 3.3 b.
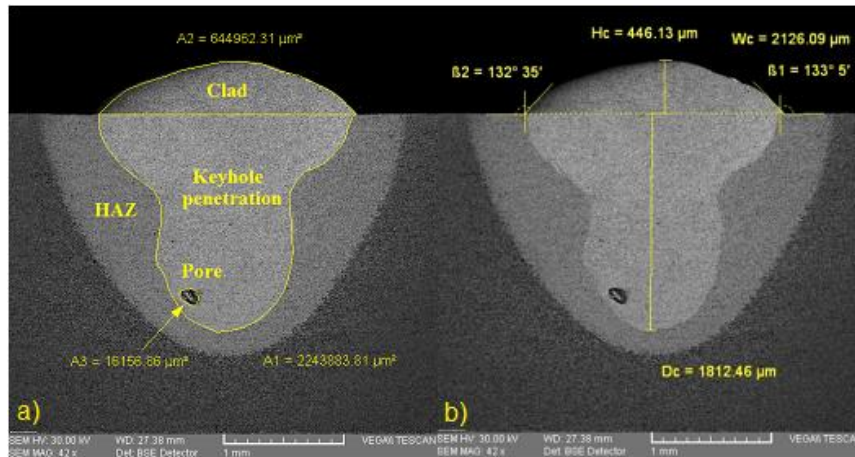
Fig. 3.3. SEM macro images of cladded beads: designation and measurements
of cross-sectional areas (a); dimensional metrology (b).

The amount of cladded material above the substrate can be characterized by the shape parameter *WH*, obtained by multiplying the height and width parameters of the single bead ($WH = W_C \cdot H_C$). As a result, the maximal value (1.6 mm^2) corresponds to a lower value of cladding speed (600 mm/min) and a defocusing distance in the range of –2...–1 mm (Fig. 3.4 a). In general, the greatest effect on this characteristic is caused by the cladding speed, showing a very similar tendency of data reduction as the speed increases (Fig. 3.4 b).
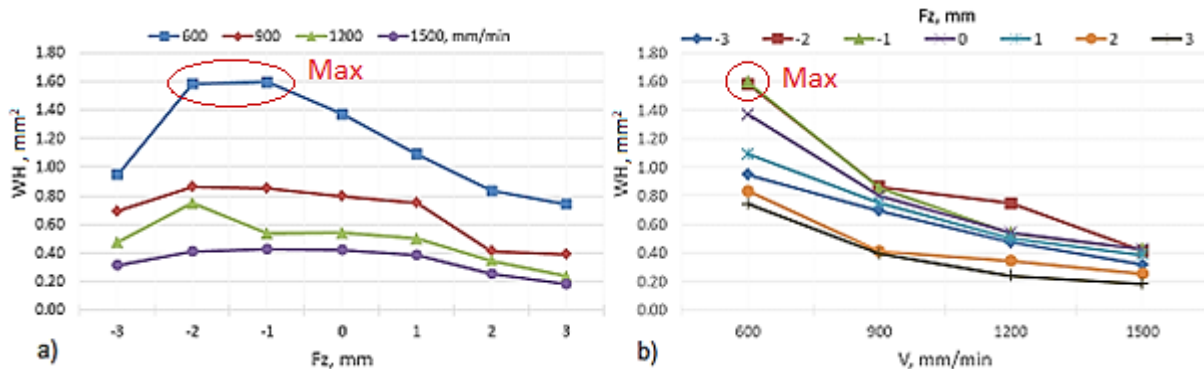

Fig. 3.4. Changes in shape parameter (*WH*): depending on the laser beam
focus shift (a); depending on the cladding speed (b).

Relative to the penetration depth and contact angle of the clad bead, the laser beam defocusing parameter has the greatest effect on it (Fig. 3.5 a). The minimum depth of the penetration was about 1 mm, which was achieved at the largest defocusing distance (+3 mm) and at higher regimes of cladding speed (900–1500 mm/min). In its turn, the largest depth of the penetration (2.3–2.5 mm) corresponded to the focus position closer to the surface treated (– 1...+ 1 mm) and was deeper at lower cladding speed. The contact angle values for all beads were in the range of 17–67°, which satisfies the clad forming condition ($\theta < 90°$). Smaller values of the contact angle corresponded to larger defocusing distance (+3 mm) and highest speed regimes (900–1500 mm/min), while the highest values were mainly concentrated at the focus positions: –1...0 mm (Fig. 3.5 b).
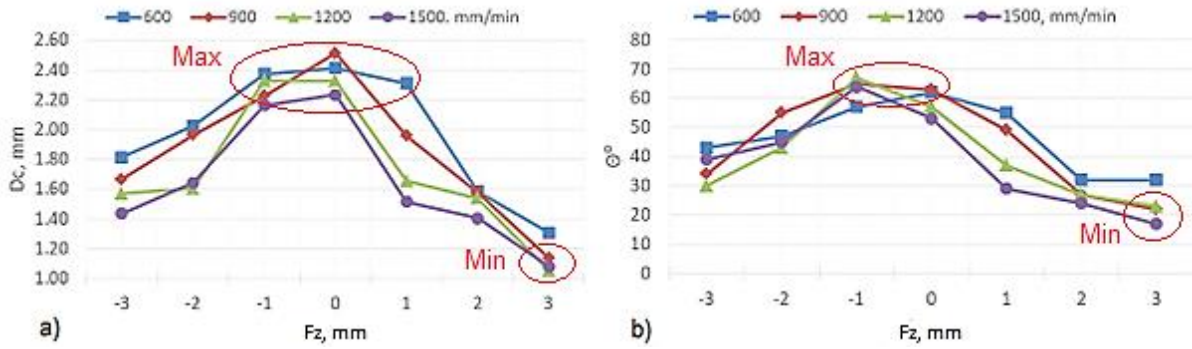
Fig. 3.5. Changes in the depth of penetration D_C (a);
and the contact angle θ vs. focus shift (b).

The highest amount of carbide-forming elements (Cr, W, Mo, V) (6.2 wt. %) corresponds to defocusing distance of −1 mm and lower cladding speed (600 mm/min) (Fig. 3.6 a). The change in porosity depending on the process parameters was mostly stochastic, however, the highest pore concentration (9 %) corresponded to the combination of higher cladding speed (1500 mm/min) and +1 mm defocusing distance, whereas the average pores concentration of beads was 2 %. In contrast, when cladded with laser beam focus shift: −1; 0 and +3 mm, the beads were practically without pores (Fig. 3.6 b).
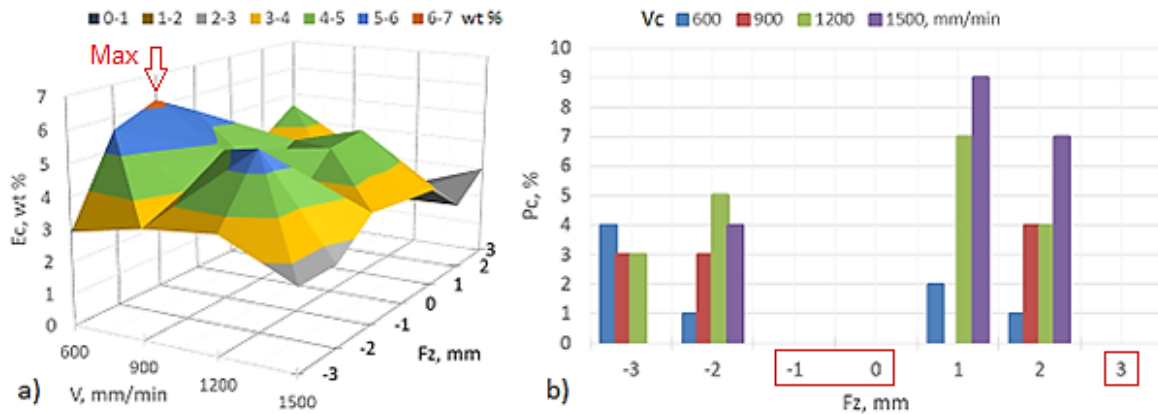

Fig. 3.6. The character of the change in quality criteria depending on process parameters:
amount of carbide-forming elements (Cr, W, Mo, V) (a); porosity (b).

Regression analysis revealed statistically significant linear relationships between process technological parameters (F_Z – defocusing distance and V – cladding speed) and geometric parameters of bead shape (H_C – cladded bead height; W_C – width; D_C – penetration depth; θ – contact angle) in both beam defocusing directions, with an exception: the cladding speed has negligible influence on the contact angle in the case of negative defocusing. As a result, linear regression models of bead geometry parameters were obtained with mean absolute percentage error ($\bar{A}_\varepsilon$) in the range: 4–13 %. Significant linear dependence was determined between the amount of carbide-forming elements and the process parameters, except for the focus shift parameter in the negative defocusing direction; while the developed regression models $\bar{A}_\varepsilon$ make up 16–17 %.

4. Study of Quality Characteristics and Properties of Laser Cladded Coatings With Keyhole in Penetration

In this chapter, the process of forming coatings with keyhole in penetration depending on the basic parameters of the laser cladding process (overlap ratio OR, %; cladding rate V, mm/min; metal powder consumption F_P, g/min) is discussed.

Experimental materials, settings and planning

High-speed steel coatings were cladded onto 41Cr4 and C80U steel substrates. The experimental work was carried out according to the full factorial experiment (FFE) design 2^3, which allows to evaluate all linear effects. Levels of experimental factors and intervals of variation are shown in Table 4.1.

Table 4.1

Factor Levels and Variation Intervals

Factor, unit	Designation	Factor levels		
		High (+1)	Nominal (0)	Low (−1)
Overlap ratio, %	OR	50	40	30
Cladding speed, mm/min	V	1500	1200	900
Powder consumption, g/min	F_P	10	7.5	5

Other process parameters in the experimental work were constant values for each coating, similar to the first experiment, with the exception of such parameters as laser beam defocusing: −1 mm and base material preheating temperature: 250 °C.

Based on the experimental data, regression analysis was performed and empirical prediction models are developed, which are characterized by the response function

$$Y_i = f(OR, V, F_P), \qquad (4.1)$$

where the following characteristics were taken as the response variables Y_i: H_E − effective thickness of the cladded layer, mm; D_P − depth of penetration, mm; E_P − amount of carbide-forming elements (Cr, Mo, W, V) in the clad, wt. %.

The effect of heat treatment (600 °C, 2 h) on the mechanical properties of the coatings was also analysed.

Main results and Conclusions of the Experiment

Figure 4.1 (a) shows one of the cross-sections of the coating. The coating system is conditionally divided into three zones: clad zone (CZ), interface zone (IZ), and keyhole penetration zone (KPZ).

The microstructure of the coating has a mixed grain structure: the cellular and dendritic grain formations based on the martensite matrix and the network of austenitic-carbide eutectic at the grain boundaries were evident (Fig. 4.1 c). Areas near the upper surface are predominantly cellular microstructure. The central area of the bead contains mostly equiaxed dendrites, but next to the interface zone with the substrate and pre-cladded beads, first and

second order columnar dendrites (Fig. 4.1 d). The finest graininess corresponds to the coatings obtained at the highest cladding speed and the lowest overlap ratio.

The presence of pores and micro-cracks within cross-sections of some of the coatings was detected. Individual cracks were observed mainly in coatings that were cladded at the highest powder mass feed rate, mostly in combination with C80U steel base material. In addition, the use of heat-treatment to prevent this type of defect is ineffective. For coatings cladded at the lowest powder feed rate (5 g/min), no cracks were found. The pores were mostly located near the peaks of keyhole penetration.
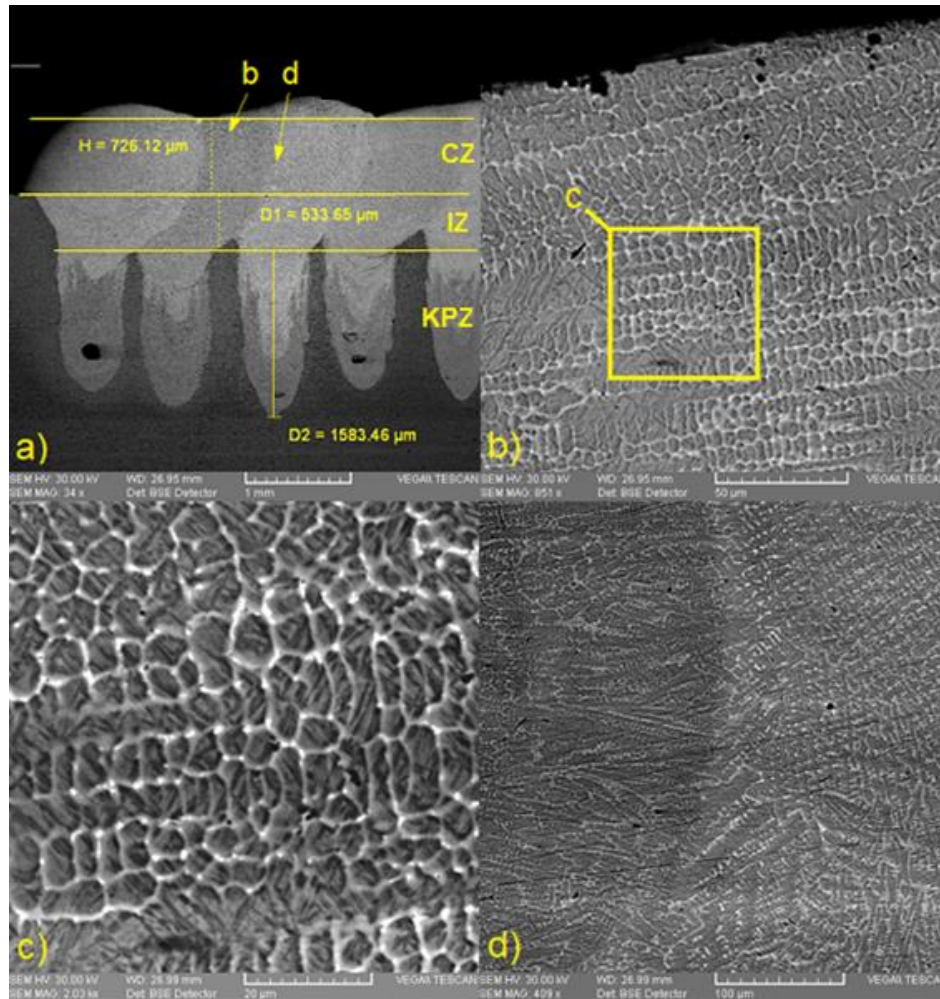

Fig. 4.1. Morphology of the coating cross-section (substrate 41Cr4, Regime 5):
CZ – clad zone; IZ – interface zone; KPZ – keyhole penetration zone.

The average values of the effective thickness of the cladded coatings according to the combinations of technological parameters varies in the interval of 0.21–0.73 mm and, as can be seen in Fig. 4.2 (a), the thickness of the coatings for base material of both types has practically identical changes. The thickness of the coating decreases as the cladding speed increases and the spacing between adjacent beads increases. Consequently, a fairly similar tendency in data reduction for powder feed rate can be seen. The maximal coating thickness corresponded to Regime 5 of the experimental design ($OR = 50$ %, $V = 900$ mm/min; $F_P = 10$ g/min).

The following regression models describe the relations between coating thickness and technological parameters (Table 4.2).

Coating Thickness Regression Models

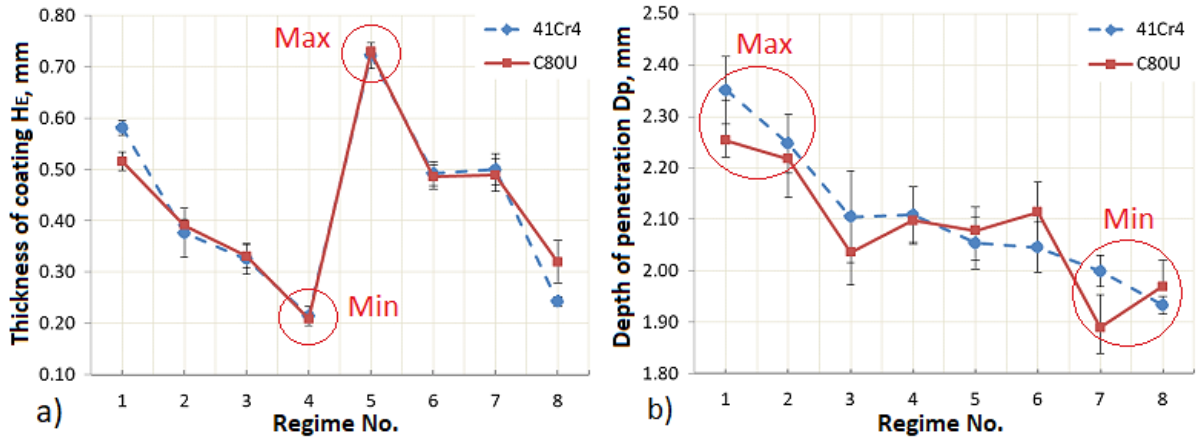| Steel	Regression equations	R^2	$\bar{A}_\varepsilon$
41Cr4	$H_{E1} = 0.3031 + 0.01003\,OR - 0.00037\,V + 0.02285\,F_P$	0.97	8 %
C80U	$H_{E2} = 0.2741 + 0.00823\,OR - 0.00032\,V + 0.02884\,F_P$	0.97	5 %

Fig. 4.2. Changes in form parameters of coating depending on process regimes:
a) thickness of the coatings; and b) depth of penetration.

The average values of the total penetration depth ($D_P = D_1 + D_2$) of the formed coatings are in the range of 1.9–2.4 mm. The highest values of the penetration depth correspond to the first two regimes, namely the minimal depth corresponds to the last two regimes (Fig. 4.2 b), which mainly determines the changes in cladding speed and powder feed rate.

The regression models in Table. 4.3 show the character of the parameter effects on the two types of steel used.

Regression Models of Coating Penetration Depth

Steel	Regression equations	R^2	$\bar{A}_\varepsilon$
41Cr4	$D_{P1} = 2.586 + 0.00219\,OR - 0.000230\,V - 0.03895\,F_P$	0.92	1 %
C80U	$D_{P2} = 2.696 - 0.00178\,OR - 0.000279\,V - 0.02758\,F_P$	0.96	1 %

Changes in the amount of carbide-forming elements (Cr, Mo, W, V) in the coatings depending on the process parameter combinations were evaluated in the EDS analysis. As a result, the amount of alloying elements in the cladded layer was reduced by 47–75 % compared to the amount of these elements in the metallic powder (16.3 wt. %).

The diagram in Fig. 4.3 (b) shows the character of the change in the amount of carbide-forming elements depending on the process regime. As it can be seen, with the increase in powder feed rate, the amount of carbide-forming elements increases significantly. The highest amount of elements (8.5–8.6 wt. %) corresponds to Regime 5 of the experimental design matrix.
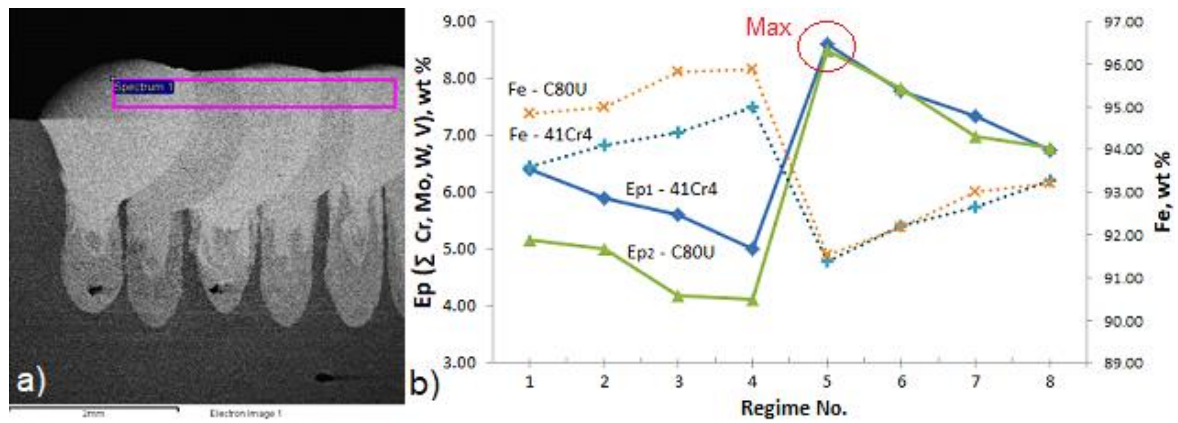
Fig. 4.3. Marked area in the cross-section of the coating for EDS analysis (a); character of the change in the quantity of elements depending on the process regimes (b).

Comparison of this graph with the characteristic curves of the coating thickness change shows a very similar pattern of change: in both powder feed rate groups (5 g/min and 10 g/min), the amount of alloying elements decreases by increasing both cladding speed and spacing between adjacent beads.

In Table 4.4 the obtained regression models are presented. Signs of each coefficient show that with increase of the powder feed rate and the overlap ratio of the beads, the amount of carbide-forming elements in the coating increases. Similarly, as in the case of single bead cladding, by increasing the cladding speed the amount of alloying elements in the clad is reduced.

Table 4.4

Regression Models of the Amount of Coating Carbide-forming Elements (Cr, Mo, W, V)

Steel	Regression equations	R^2	$\bar{A}_\varepsilon$
41Cr4	$E_{P1} = 4.569 + 0.0318\,OR - 0.0017\,V + 0.3778\,F_P$	0.99	1 %
C80U	$E_{P2} = 3.392 + 0.0132\,OR - 0.0018\,V + 0.5799\,F_P$	0.99	2 %

Since many materials are known to have an interrelationship between hardness and strength criterion [40], [41], the change in hardness values in the cross-section of the coating indirectly reflects the character of the change in the mechanical properties of the material. For this purpose, the analysis of the change of microhardness in the cross-sections of the non-crack coating group was carried out by making measurements in the normal direction from the surface of the coating to the substrate (Fig. 4.4).

The hardness of the surface layer varies between 830 and 500 HV 0.2. Thus, depending on the process regime, the increase in microhardness of the coated surface can make from 70 % to 250 % compared to the microhardness of the untreated base material (41Cr4 steel – 240 HV 0.2, C80U steel – 290 HV 0.2). Basically, higher microhardness values correspond to coatings with higher overlap ratios (50 %) and lower speed (900 mm/min), regardless of the type of the base steels (Fig. 4.4 b–d). This result is in good agreement with the previously obtained amount of carbide-forming elements in the coatings, i.e. coatings with the highest amount of alloying elements are generally of the highest hardness.

The obtained curves of microhardness change are grouped by cladding speed values and include the microhardness curves (profiles) of the coatings that were cladded to both substrate steel types (41Cr4 in Fig. 4.4 b, c and C80U in Fig. 4.4 d, e). The profiles shown are divided by the overlap ratio (OR 50 % and OR 30 %), with solid lines for non-heat-treated coatings and dashed lines for heat-treated coatings (HT), respectively.
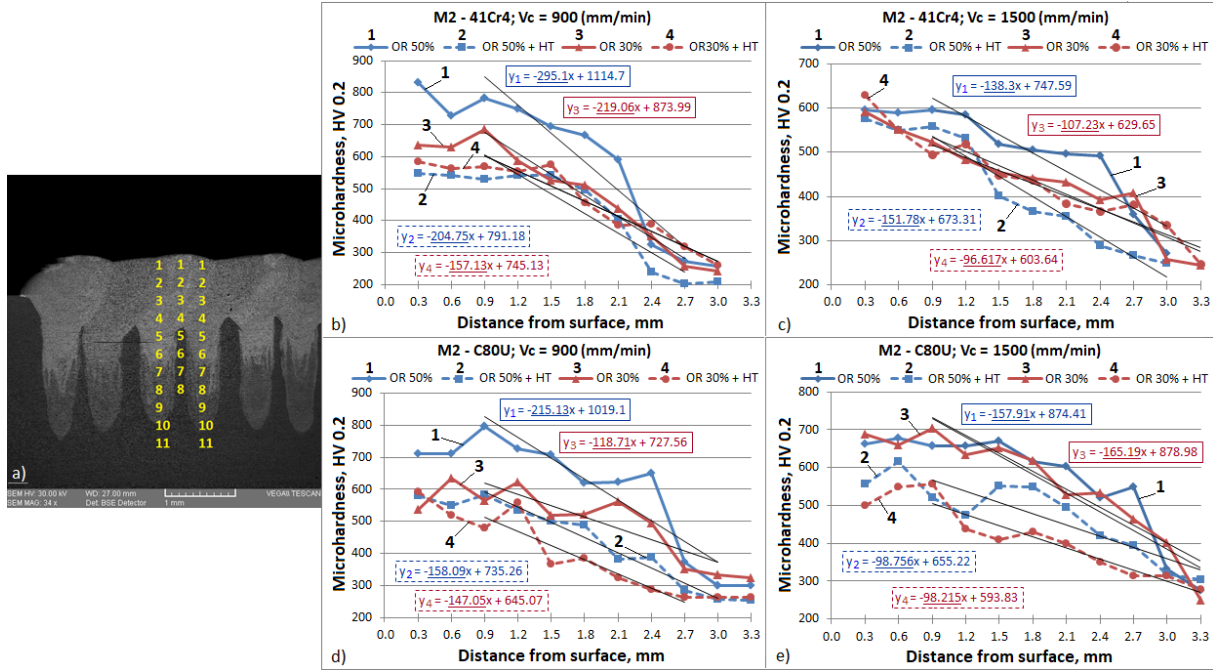

Fig. 4.4. Characteristics of the microhardness change in the coating-substrate system:
a schematic representation of the implementation of the measurements (a); microhardness profiles of the respective regimes in different combinations of coating (AISI M2) and base material (41Cr4 and C80U) (b–e).

As can be seen, heat treatment generally leads to a significant reduction in microhardness (Profiles 2 and 4). However, these characteristics show a smoother transition of hardness to the substrate. Furthermore, it was found that the microhardness profiles corresponding to coatings with the lowest overlap ratio of 30 % (Profiles 3) generally exhibit very similar characteristics to HT profiles.

Linear trends with regression equations were created to represent the microhardness gradient of the created coatings, where the slope coefficients reflect the nature of the microhardness change in the coating and substrate transition area. Based on the equation coefficients, the values of the microhardness gradients for non-heat-treated coatings are in the range of 107–295 HV/mm, whereas for heat-treated coatings this characteristic is generally lower: 97–205 HV/mm. As a result of the research, the regimes with the lowest microhardness gradient in the coating-substrate system without the application of heat treatment were determined. Thus, the realization of the proposed laser cladding method in regimes that provide the smallest gradient will, firstly, shorten the production process cycle, eliminating the need for heat treatment and, secondly, reduce the risk of coating cracking.

5. Study of the Anizotropical Effect on Laser Cladded Coatings Surface Properties After Machining

Due to the discrete deposition of coatings, they exhibit heterogeneity of structure in the transverse direction of the clad. As a result, the anisotropic structure of coatings may affect the character of the functional properties of the surface. As a result, the cladded surface has a high degree of waviness and surface roughness (Fig. 5.1), therefore, in order to ensure the required surface quality, all laser cladded coatings must undergo post-cladding machining – often by using grinding. In contrast, conventional abrasive wheel grinding, due to the wavy texture of the coating, may result in varying of the force applied to the tool and detail, which due to unwanted vibrations can cause traces of vibration, surface burns, micro-cracks and unwanted tensile stresses, which may negatively affect the surface properties of fine finished coatings [42], [43].
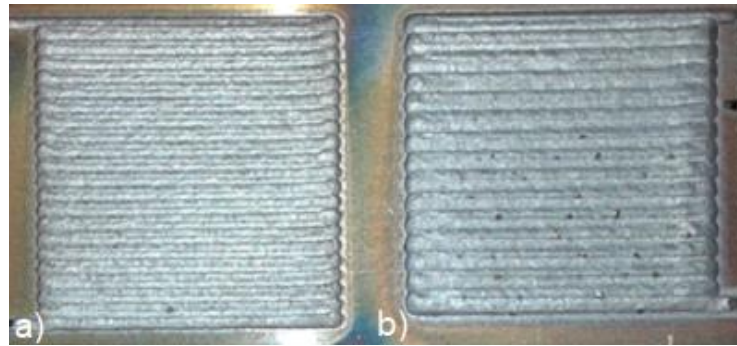

Fig. 5.1. Laser cladded coatings in different regimes:
cladding speed values: 1200 mm/min (a); 600 mm/min (b).

Therefore, in this chapter, the effect of process regime on the properties of coatings was analysed using different processing strategies that include different mutual orientations in the direction of the cladding and grinding processes. Such conditions may occur when the coatings are applied to the cylindrical surfaces of the items, along the body rotation direction (Fig. 5.2 a) or when the coating is applied axially (Fig. 5.2 b). In contrast, surface grinding after laser cladding is performed in the direction of body rotation.
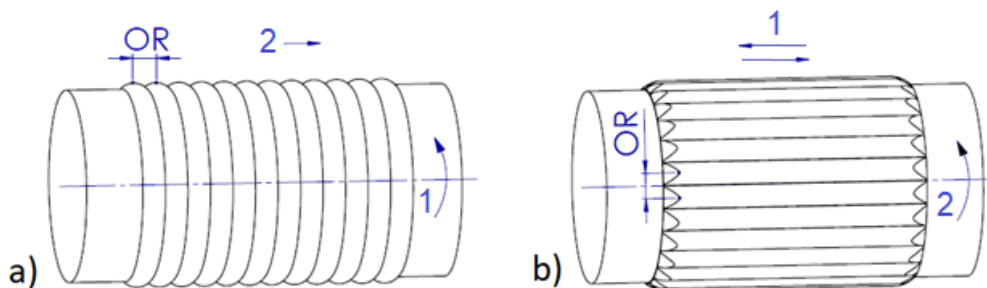

Fig. 5.2. Schematic representation of laser cladding techniques for rotating surfaces:
circumferential laser cladding (a); axial laser cladding (b);
1 – direction of cladding; 2 – direction of single bead overlap; OR – overlap ratio.

Experimental Materials, Settings and Planning

During the experiment, two coating groups were laser cladded on spring steel (DIN 66Mn4) sheets according to the experimental design in step with the process parameter combinations. In the next step, the 1st group of coatings were flat grinded along the direction of the cladded beads and the 2nd group of coatings were grinded transversely to the direction of the cladded beads.

Experimental high-speed steel coatings were designed according to FFE plan 2^3, varying such factorial variables as: overlap ratio OR, %; cladding rate V, mm/min; and defocusing direction F_Z, mm. Factor levels and ranges of variation are given in Table 5.1.

Table 5.1

Factor Levels and Variation Intervals

Factor, unit	Designation	Factor levels		
		High (+1)	Nominal (0)	Low (−1)
Overlap ratio, %	OR	50	43	35
Cladding speed, mm/min	V	1200	900	600
Direction of defocusing, mm	F_Z	+2	0	−2

The following response variables (Y_i) were chosen for the quality assessment of coatings: H_P – coating thickness, mm; C_P – hardness of the grinded surface of the coating, HRC; μ – dry sliding friction coefficient of the surface of the coating. Regression analysis was used to construct empirical models of relationships which are described by the response function:

$$Y_i = f(OR, V, F_Z). \tag{5.1}$$

Basic Results and Conclusions of the Experiment

Visual inspection of the grinded surfaces showed that most of the samples had a qualitative surface, with no obvious defects (Fig. 5.3 a), while some of the coated surfaces had pores (Fig. 5.3 b).
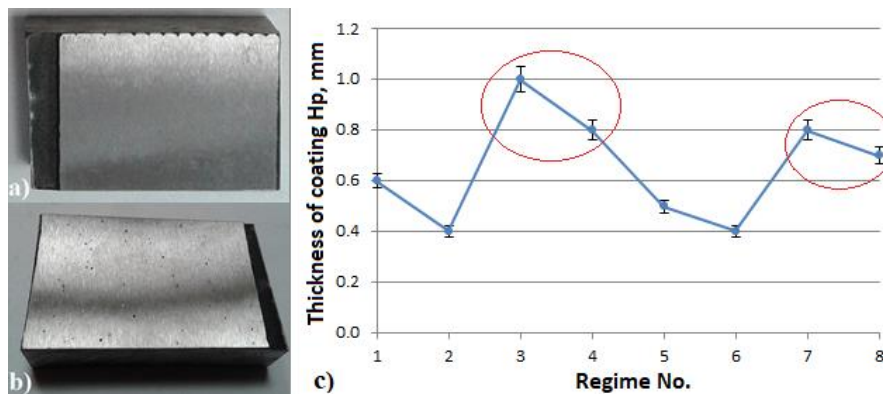

Fig. 5.3. Coating surfaces after grinding: without defects (a); porous (b);
variation in coating thickness depending on process regimes (c).

24

The thickness of the as-cladded layer varies from 0.4 mm to 1 mm. Diagram in Fig. 5.3 (c) shows that the highest coat thicknesses (0.7–1 mm) correspond to Regime 3, 4, 7, and 8, which are united by the lowest speed (600 mm/min).

As a result of regression analysis, an empirical model (Eq. (5.2)) of laser cladding process was obtained. It describes the linear relationship of coating thickness with technological parameters of the process. This equation shows that the coating thickness increases with increasing coating rate but decreases with increasing cladding rate and defocusing distance. The coefficient of determination $R^2 = 0.97$ and the mean absolute percentage error $\bar{A}_\varepsilon < 5$ % indicate high quality of the regression model and mathematical accuracy.

$$H_P = 0.75 + 0.01\,OR - 0.000583\,V - 0.025\,F_Z. \qquad (5.2)$$

The diagram in Fig. 5.4 represents the changes in hardness data (HRC) for both groups of grinding directions according to the order of cladding regimes. As can be seen, the highest hardness (over 65 HRC) corresponds to Regime 4, 7, and 8. Meanwhile, the variation of the values between the grinding directions is insignificant – their difference mostly fluctuates within 1 HRC. Thus, it was found that the direction of grinding did not significantly affect the changes in the hardness values of the coatings.
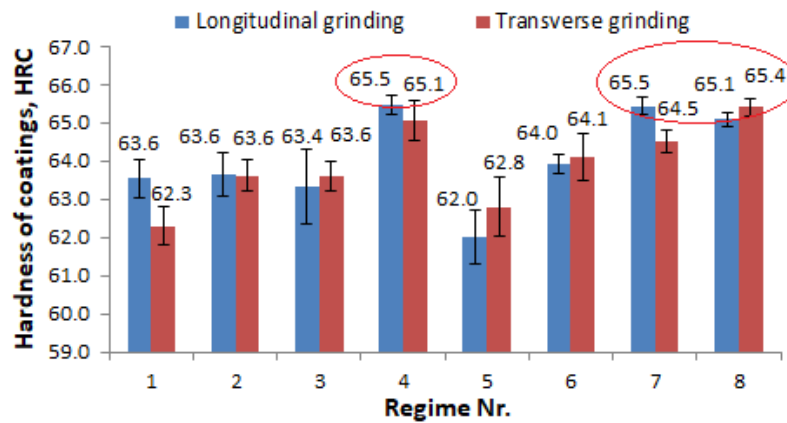

Fig. 5.4. Changes in hardness of grinded coatings surfaces depending on process regime.

The regression models (Table 5.2) characterize the relationship between the hardness of the coatings and the process parameters corresponding to the different directions of grinding. In this way, one can see that the surface hardness decreases with increasing overlap ratio and cladding speed, while increasing of the defocusing distance induces an increase in surface hardness.

Table 5.2

Coating Hardness (HRC) Regression Models

Grinding direction	Regression equations	R^2	$\bar{A}_\varepsilon$
Longitudinally	$C_{P(G)} = 69.05 - 0.0625\,OR - 0.00258\,V + 0.027\,F_Z$	0.65	1 %
Transversely	$C_{P(S)} = 69.64 - 0.0833\,OR - 0.00241\,V + 0.141\,F_Z$	0.99	1 %

Dispersion analysis showed that corresponding to obtained linear regression models, high statistical significance is only in case of the transverse grinding. Meanwhile, the average absolute percentage error for the two models created does not exceed 1 %.

In the second step, in order to evaluate the effect of coating anisotropic structure on the character of the change in mechanical properties, a microhardness change character analysis on the post-machined surface of the coating in two perpendicular directions was performed. Figure 5.5 shows one of the samples the surface of which was fine grinded and polished to a mirror smooth surface condition ($Sa = 0.015$ µm).
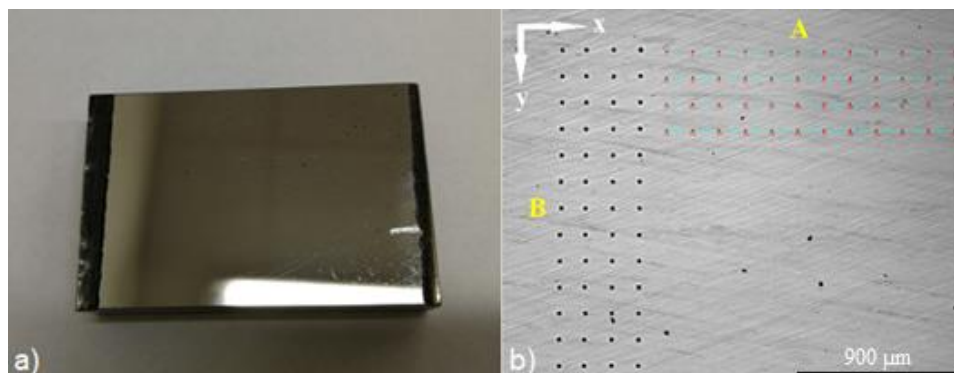

Fig. 5.5. Specimen with polished surface (a); arrangements of measuring point arrays (b): A – transverse to the orientation of the cladded beads, B – longitudinal to the orientation of the cladded beads (distance between points: 150 µm × 150 µm).

As can be seen from the diagrams in Fig. 5.6, there is a nonuniformity of microhardness data in both directions, values obtained irregularly fluctuate around 900 HV 0.2 mark, where the maximum value of transverse distribution was 9 % and longitudinal 12 %, respectively. In addition, when looking at the transverse curve (A-curve), it is not observed that changes in the microhardness in the transverse direction of the cladded beads reflected repeatability in the order of data variation that would result from the repeated interchanging of different structures. Fluctuations of microhardness in the longitudinal direction (B-curve) can also be observed, and the periodicity is not regular as well.
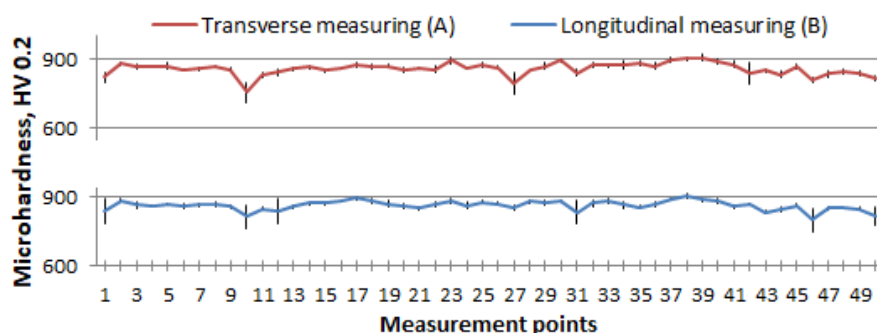

Fig. 5.6. Microhardness distributions on the surface of the coating in interperpendicular directions (distance between measuring points 150 µm).

Thus, judging by these characteristics, it is not possible to assert univocally that the coating surface has anisotropy of properties, since there is uncertainty in the change of data in

both directions of measurement. Such character is probably due to the specificity of the cladding process, namely: the single bead cladding process has a certain degree of stochasticity due to the associated co-process irregularity – the state of powder particles in the gas powder stream and their order of entry in the molten pool.

Testing of coating friction coefficient showed that the different regimes of laser cladding process produce different effects on both friction coefficient and counter-body (ball) surface abrading. As a result of the experiments, the best combination of technological parameters was determined – Regime 5 ($OR = 50$ %, $V = 1200$ mm/min; $F_Z = +2$ mm), where the lowest value of the friction coefficient ($\mu = 0.16$–0.21) was obtained, which is twice as low as the friction coefficient of the base material.

Figure 5.7 shows the results of the friction test experiment, that is, the mean value of the friction coefficient and the changes in the abraded surface areas of the ball in accordance with the coatings developed for the respective regime settings. The ordinates of the graph represent the values corresponding to the base material – grey horizontal lines show the reference or base values, which represent the values of the friction coefficient of the base material ($\mu = 0.469$) and the abraded surface area of the ball ($S_L = 0.123$ mm^2).

In general, the graphs have fairly similar distribution patterns, where the values of the friction coefficients of both grinding directions fluctuate in different directions close to the baseline, but equally represent the significant reduction of the friction coefficient on coatings created after Regime 5 settings. Consequently, the abraded surface area of the ball shows a similar pattern of data change.
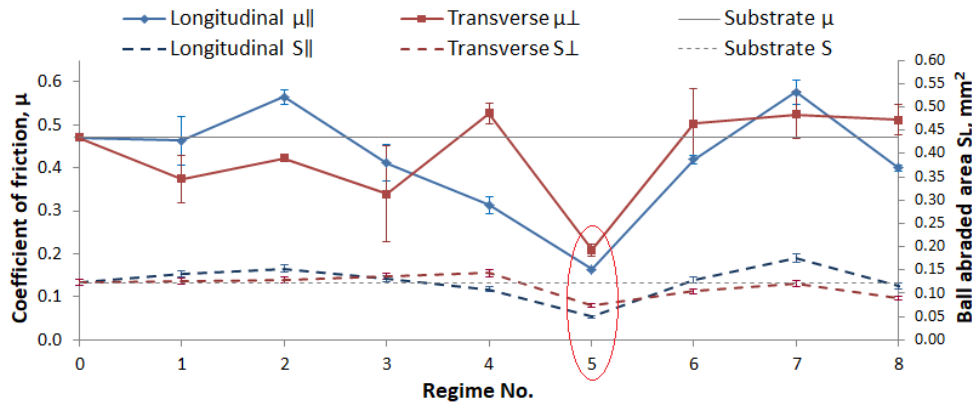

Fig. 5.7. Changes in friction coefficient and ball wear surface area with respect to the order of regimes for longitudinal and transverse grinding directions.

Comparing the mean values of the friction coefficients between the two groups of grinding directions, it was determined that these values are in fact equivalent, respectively: for the longitudinal data set the mean value of the friction coefficient is $\bar{\mu}_{\parallel} = 0{,}414$, and for the transverse data set $\bar{\mu}_{\perp} = 0{,}426$.

As a result, considering the friction coefficient results along with the character of the change in hardness, laser cladded coating surfaces generally exhibit a certain degree of homogeneity with a relatively probable character. Thus, the mutual orientations of the cladding and grinding directions have a negligible influence on the hardness of the coatings and changes in the friction coefficients.

6. Comparative Analysis of Differently Laser Cladded Coatings

In this chapter, the properties of coatings created by two different laser cladding methods were considered. For this purpose, two coating groups were cladded: one coating group using conventional laser cladding technology, which provides minimum penetration of the base material; and the other coating group – cladded according to the method proposed in this work, forming keyhole in penetration.

Experimental materials, settings, and evaluation methods

Experimental coatings (high-speed steel AISI M2) were cladded onto tool steel AISI D2 sheets with a nominal hardness of about 255 HB (ISO 18265: ~268 HV, ~25 HRC).

In order to achieve different size of penetrations, the coatings were cladded using two different regimes, the main difference being laser beam power density maximum. Thus, for the 1st group of coatings $I_0 = 1.95 \cdot 10^3$ W/mm^2, whereas for the 2nd group of coatings $I_0 = 4.87 \cdot 10^3$ W/mm^2.

Research on the prepared coatings was performed on cross-sectional microspecimens by comparing the morphology of the coatings, the amount of carbide forming elements (Cr, Mo, W, V) in the cladded layer, changes of mechanical properties according to the microhardness distribution in the cross sections of coatings, as well as tribotechnical properties of mirror polished coatings surfaces ($Sa = 0.015$ µm).

Basic results and conclusions of the experiment

The average effective thickness (H_E) of the cladded layers for the 1st group of coatings is about 650 µm and for the 2nd group of coatings about 380 µm respectively (Fig. 6.1). The depth of the penetrations (D_P) is about 210 µm for the 1st group and, for the 2nd group, the average depth of the penetrations ($D_P = D_1 + D_2$) is about 1625 µm. Consequently, some pore inclusions are found in the 2nd group of coatings, as observed in previous studies, along the keyhole in penetration axis, mostly closer to its root.
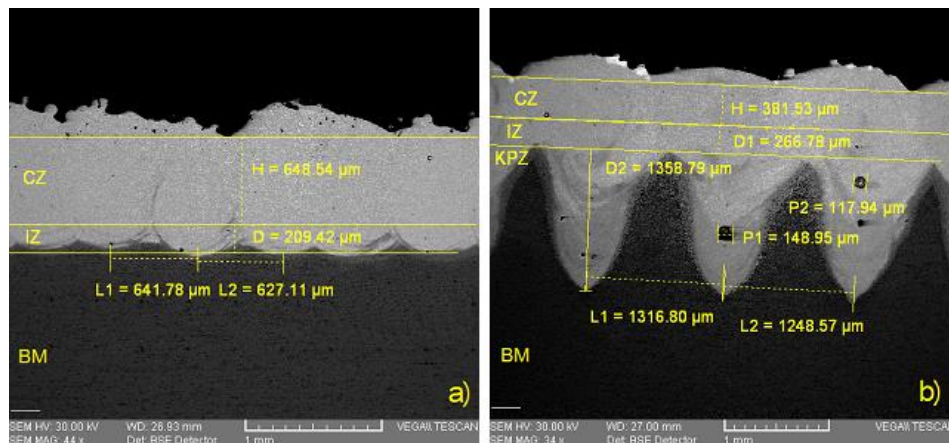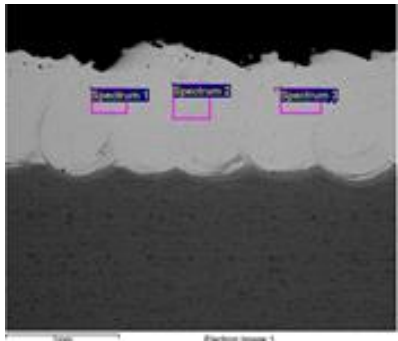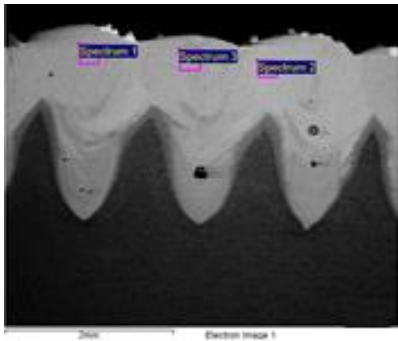

Fig. 6.1. The 1st group (a) and the 2nd group (b) of coatings cross-sectional views with geometric measurements.

The EDS analysis showed that the amount of carbide-forming elements (Cr, Mo, W, V) in the 1st group of coatings is practically similar to that of the original powder (Table 6.1). On the other hand, in the 2nd group of coatings, the amount of Mo, W, V in the cladded layer was reduced almost two times and thus contained more Cr and Fe. Thus, this analysis showed that the dilution ratio is highest for the 2nd group of coatings. As a result, it was determined that the greatest depth of the penetration results in the greatest degree of mixing between the coating and the base material.

Table 6.1

Results of EDS Analysis (Average Element Content, wt. %)

The 1st group of coatings					The 2nd group of coatings				
V	Cr	Mo	W	Fe	V	Cr	Mo	W	Fe
2.06	4.74	5.26	5.66	80.40	1.35	8.71	1.35	2.45	82.90

The characters of the changes in the mechanical properties of the coatings are reflected in the following 3D microhardness diagrams. As can be seen in Fig. 6.2, coatings of the 1st group exhibit a fairly even change in the beads overlap direction (X-axis on the graph). However, in the direction of the material depth (Y-axis), the microhardness shows a sharp drop from 900 HV 0.2 to 250 HV 0.2. In contrast, coatings of the 2nd group exhibited heterogeneity of properties along the X and Y axes with microhardness peaks in 0.7 mm depth corresponding to the cavities between adjacent keyhole-shaped penetrations (Fig. 6.2).
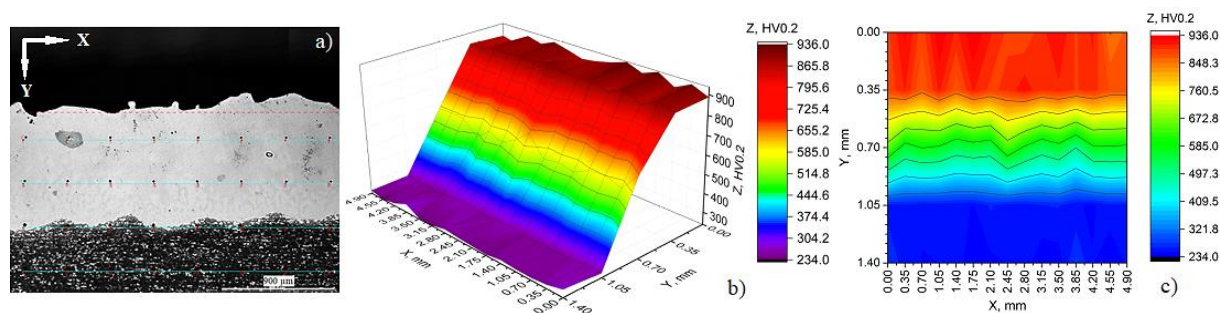
Fig. 6.2. Microhardness (HV 0.2) distribution in the 1st group of coating cross-section:
array of rectangular indentation points 350 µm × 350 µm (a);
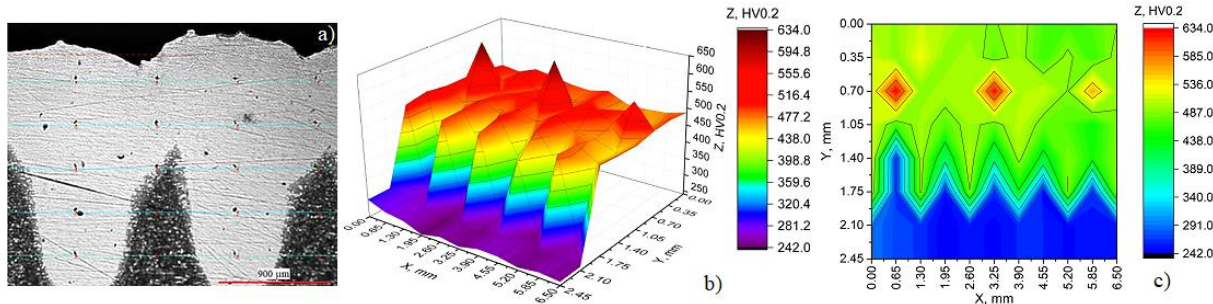3D microhardness diagram (b); 2D microhardness mapping (c).

Fig. 6.3. Microhardness (HV 0.2) distribution in the 2nd group of coating cross-section: array of rectangular indentation points 650 μm × 350 μm (a); 3D microhardness diagram (b); 2D microhardness mapping (c).

Comparison of the microhardness change profiles as a function of the change in depth coordinate from the surface to the substrate (Fig. 6.4) shows that the 2nd group of coatings exhibit a slower change in the values towards the substrate than the 1st group of coatings. The coefficients of the linear regression equations represent the magnitudes of the microhardness gradients in the transition zone of the coating and base material, namely for the 1st group of coatings: 908.56 HV/mm and for the 2nd group of coatings: 134.02 HV/mm. Thus, assuming a relationship between material hardness and stress state [44], it can be presumed that the lower the gradient of hardness, the more regular is distribution of residual stresses in coating-substrate system. Analysing the results of microhardness change it is determined that coatings with keyhole in penetration have the smallest gradient of mechanical properties in the transition zone between the coating and the base material compared to coatings with a small penetration depth. This is achieved through the alloying of near surface layers of the base material with slowly decreasing element content while increasing the depth. Thus, it is possible to approximate the difference between the properties in dissimilar steels by introducing a coating with keyhole in penetration, which may contribute to the reduction of internal residual stresses in the surface hardening coatings.
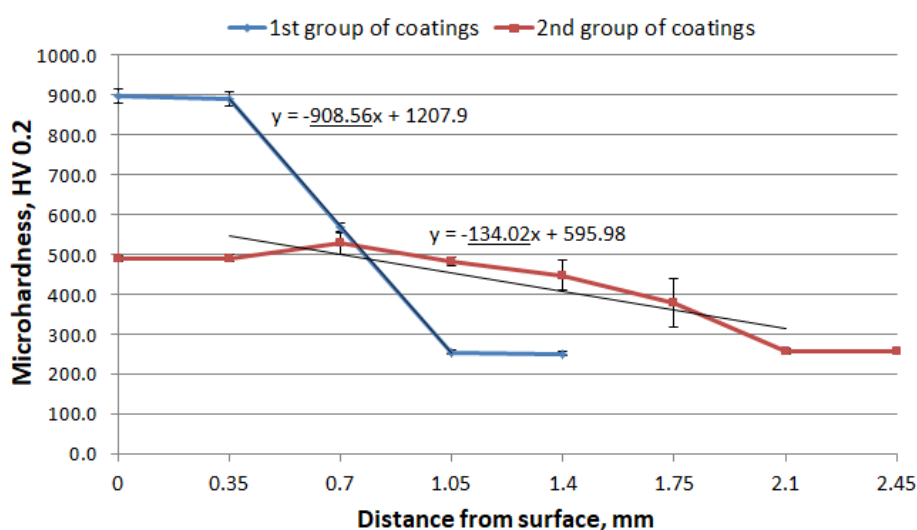

Fig. 6.4. Vickers microhardness profiles on coatings cross-sections as a function of change of depth coordinate.

30

High hardness value is often not the predominant factor for the best operational characteristics. Therefore, tribological testing of the developed coatings was performed to determine the dry sliding friction coefficients of the coatings and their changes during testing. In Figure 6.5 characteristic curves are shown for both groups of coatings. The friction curves are mainly similar in both coating groups, with the only exception in the running-in stage, where slightly coarser running-in conditions for the 2nd group of coatings were observed.
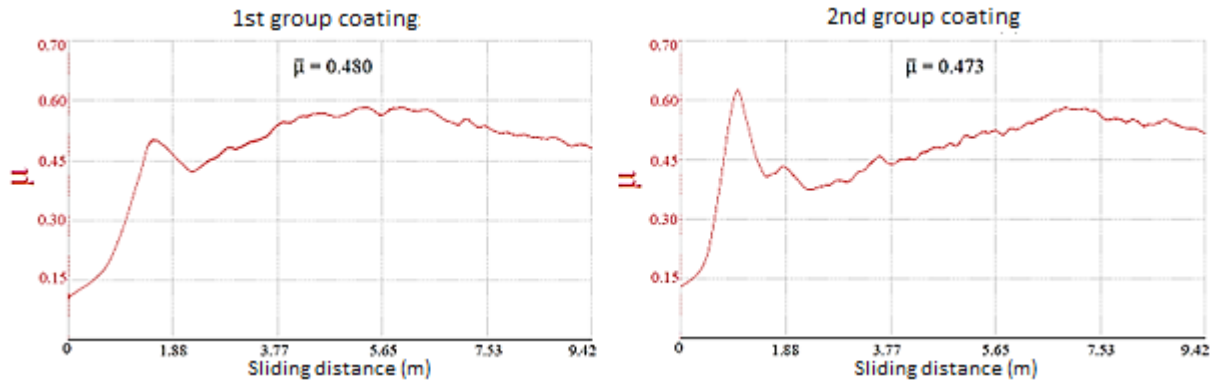

Fig. 6.5. Characteristic curves of coatings friction coefficients.

In general, the mean values of the friction coefficients are virtually equivalent, namely: for the 1st group of coatings this value is $\bar{\mu} = 0.511$, and for the 2nd group of coatings $\bar{\mu} = 0.503$ respectively.

As a result, it was found that the two groups of coatings have virtually similar tribotechnical properties regardless of the variability of the surface layer hardness. The results obtained in sliding friction coefficient testing are summarized in Table 6.2.

Table 6.2

Friction Coefficient Test Results for Differently Laser Cladded Coatings

Name of the parameter	Designation of parameter	1st group of coatings	2nd group of coatings	Base material
Mean value of the friction coefficient	$\bar{\mu}$	0.512	0.503	0.536
Maximum value of the friction coefficient	μ_{max}	0.675	0.631	0.922

MAIN RESULTS AND CONCLUSIONS OF THE STUDY

1. In the study of the nature of changes of quality characteristics of laser cladded high-speed steel (AISI M2) beads with keyhole in penetration, the regime ($V = 600$ mm/min, $F_Z = -1$ mm) was determined, where the highest amount of cladded material (1.6 mm^2), highest amount of carbide-forming alloys (Cr, Mo, W, V) in the clad (6.2 wt. %) and minimal porosity was reached.

2. Empirical models of relationships of the quality characteristics of laser cladded bead and technological parameters were obtained, which allows to have control over the geometric parameters of the single bead's shape and the amount of carbide-forming elements (Cr, Mo, W, V). Approximation error values of linear regression models for the shape parameters were 4–13 %, and for the amount of carbide-forming elements 16–17 %.

3. Experimentally were determined areas of laser cladding process regimes ($I_0 = 4.87 \cdot 10^3 \dots 7.73 \cdot 10^3$ W/mm^2, $V = 600\dots1500$ mm/min), which ensure the formation of cladding with keyhole shaped penetration in base material, thus creating a gradient of mechanical properties in the coating-substrate system.

4. As a result of the research, it was determined that laser cladding of non-cracked high-speed steel (AISI M2) coatings can be achieved within the microhardness gradients range of 107–295 HV/mm without the application of heat treatment.

5. Regression analysis of experimental data resulted in linear relationships between technological parameters (overlap ratio, cladding speed and powder feed rate) and coating characteristics (thickness, penetration depth, amount of carbide-forming elements), which revealed the influence of parameters and enabled obtaining prediction models of quality characteristics with a high approximation accuracy (mean absolute percentage error of up to 8 %).

6. As a result of the experimental study, the regimes of laser cladding process with the maximum hardness value (~66 HRC) were determined. Laser cladding of high-speed steel coating increased surface hardness to 288 % compared to hardness (~17 HRC) of spring steel base material (DIN 66Mn4).

7. An experimental study of the tribotechnical properties of coatings allowed determining the best laser cladding regime ($OR = 50$ %, $V = 1200$ mm/min; $F_Z = +2$ mm), which resulted in a twice lower dry sliding coefficient of friction (0.16–0.21) compared to the coefficient of friction of the spring steel base material (0.47).

8. A comparative analysis of laser cladding methods showed that although laser cladding in keyhole penetration regime contributes to the reduction of microhardness in the cladding layer, the lowest microhardness gradient (6.8 times) was obtained in the coating to substrate transition zone, in addition the tribotechnical properties were maintained at a high level.

9. The developed laser cladding method enables to create a coating with a gradient of mechanical properties in the coating-substrate system, which can favourably influence the redistribution of residual stresses when using materials with different coefficients of thermal expansion. Thus, this method simplifies the technological process of laser cladding by eliminating the need for interlayer application as well as post heat treatment in the cladding of dissimilar steels.

REFERENCES

1. Schneider, Marcel. *Laser cladding wth powder*. Ph.D. Thesis University of Twente, Enschede: Print Partners Ipskamp, 1998, 177 p. ISBN 90 365 1098 8.

2. Toyserkani, E., Khajepour, A., Corbin, S. *Laser Cladding*. *New York*: CRC Press LLC, 2005. 263 p. ISBN 0-8493-2172-7.

3. Weisheit, A., Gasser, A., Backes, G., Jambor, T., Pirch, N., Wissenbach, K. Direct Laser Cladding, Current Status and Future Scope of Application. In: *Laser-Assisted Fabrication of Materials.* J. D. Majumdar, I. Manna, ed. Berlin: Springer, 2013, pp. 221–240. ISBN 978-3-642-28359-8.

4. Pinkerton, A.J., Wang, W., Li, L. *Component Repair Using Laser Direct Metal Deposition*. In: *Proceedings of the Institution of Mechanical Engineers, Part B: Journal of Engineering Manufacture*, vol. 222, no. 7, pp. 827–836. *ISSN 2041-2975.* DOI: 10.1243/09544054JEM1008.

5. Xue, L. Laser consolidation: a rapid manufacturing process for making net-shape functional components. In: *Advances in laser materials processing* J. Lawrence, J. Pou, D.K.Y. Low, E. Toyserkani, ed. Cambridge: Woodhead Publishing Ltd, 2010, pp. 492–534. ISBN 978-1-84569-981-9.

6. Boddu, M. R., Landers, R. G., Liou, F. W. Control of laser cladding for rapid prototyping – a review. In: Proceedings – Solid Freeform Fabrication Symposium 2001: SFF Symposium in Austin, Texas on August 6–8, 2001. Austin, Texas: University of Texas Press, 2001, pp. 460–467.

7. Shishkovskij, I. V. *Lazernyj sintez funkcionalno-gradientnyh mezostruktur i obemnyh izdelij*. Moskva: FIZMATLIT, 2009. 424 s. ISBN: 978-5-9221-1122-5.Altenbach, H., Sadowski, T. *Failure and Damage Analysis of Advanced Materials*. Wien: Springer, 2015. 278 p. eISBN 978-3-7091-1835-1. (in Russian)

8. Panchenko, V. Ya. (Red.). *Lazernye tehnologii obrabotki materialov: sovremennye problemy fundamentalnyh issledovanij i prikladnyh razrabotok*. Moskva: Fizmatlit, 2009. 664 s. ISBN 978-5-9221-1023-5. (in Russian)

9. Oliveira, U., Ocelík, V., De Hosson, J.Th.M. *Residual Stress Analysis in Co-based Laser Clad Layers by Laboratory X-rays and Synchrotron Diffraction Technique. Surface & Coatings Technology,* vol. 201, 2006. pp. 533–542. ISSN: 0257-8972. Available from: doi:10.1016/j.surfcoat.2005.12.011.

10. Zhao, H., Zhang, H., Xu, C., Yang, X. *Temperature and Stress Fields of Multi-track Laser Cladding*. *Transactions of Nonferrous Metals Society of China*, 2009, vol.19, pp. 495–501. ISSN 1003-6326. Available from: doi:0.1016/S1003-6326(10)60096-9.

11. Lupoi, R., Cockburn, A., Bryan, C., Sparkes, M., Luo, F., O'Neill, W. Hardfacing Steel with Nanostructured Coatings of Stellite-6 by Supersonic Laser Deposition. *Light: Science and Applications*, 2012, vol. 1, e-10. ISSN 2047-7538. Available from: DOI: 10.1038/lsa.2012.10.

12. Pleterski, M., Tusek, J., Muhic, T., Kosec, L. Laser Cladding of Cold-Work Tool Steel by Pulse Shaping. *Journal of Materials Science & Technology*, 2011, vol. 27, no. 8, pp. 707–713**.** ISSN 1005-0302. Available from: doi: 10.1016/S1005-0302(11)60130-8.

13. Pleterski, M., Tušek, J., Kosec, L., Muhič, M., Muhič, T. Laser Repair Welding of Molds with Various Pulse Shapes. *Metalurgija*, 2010, vol. 49, no. 1, pp. 41–44. ISSN 0543-5846.

14. Muhič, T., Tušek, J., Pleterski, M., Bombač, D. *Problems in Repair-Welding of Duplex-treated Tool Steels. Metalurgija*, 2009, vol. 48, no. 1, pp. 39–42. ISSN 0543-5846.

15. Pinkerton, A.J. Laser direct metal deposition: theory and applications in manufacturing and maintenance. In: *Advances in laser materials processing*. J. Lawrence, J. Pou, D.K.Y. Low, E. Toyserkani, ed. Cambridge: Woodhead Publishing Ltd, 2010, pp. 461–491. ISBN 978-1-84569-981-9.

16. Majumdar, J. D., Manna, I. Development of Functionally Graded Coating by Thermal Spray Deposition. Chapter 5. In: *Roy, M., Davim, J. P. Thermal sprayed coatings and their tribological performances.* Hershey, PA: Engineering Science Reference, 2015. pp.121–162. Available from: DOI: 10.4018/978-1-4666-7489-9.ch005.

17. Paul, S., Singh, R., Yan, W. Finite Element Simulation of Laser Cladding for Tool Steel Repair. In: *Lasers based manufacturing: 5th International and 26th All India Manufacturing Technology, Design and Research Conference, AIMTDR 2014*, India, Guawahati, December 12–14, 2014. New Delhi: Springer India, 2015, pp. 139–156. ISBN 978-81-322-2352-8.

18. Chinahov, D.A., Grigoreva, E.G. Analiz effektivnosti sposobov vosstanovleniya detalej izgotovlennyh iz vysokoprochnyh stalej. *Tehnologii i materialy*, 2015, № 4, s. 16–20. eISSN 2410-6437. (in Russian)

19. Cao, H.T. Dong., X.P., Pan., Z. *Surface Alloying of High-vanadium High-speed Steel on Ductile Iron Using Plasma Transferred Arc Technique: Microstructure and Wear Properties. Materials and Design*, 2016, vol. 100, pp. 223–234. ISSN 0264-1275. Available from: *DOI:10.1016/j.matdes.2016.03.114.*

20. Candel Bou, JJ., Franconetti Rodríguez, P., Amigó Borrás, V. Study of the Solidification of M2 High Speed Steel Laser Cladding Coatings. *Revista de Metalurgi*, 2013, vol. 49, no. 5, pp. 369–377. eISSN 1988-4222. ISSN 0034-8570. Available from: doi:10.3989/ revmetalm.1258.

21. Sherbakov, Yu.V., Kashfullin, A.M. *Sovremennye sposoby vosstanovleniya i uprochneniya detalej*. Perm: IPC «Prokrost», 2018. 191 s. ISBN 978-5-94279-393-7. (in Russian)

22. Topolyanskij, P.A., Topolyanskij, A.P. Progressivnye tehnologii naneseniya pokrytij – naplavka, napylenie, osazhdenie. *Actual Conference*, 2011, № 4(73), s. 63–68. Pieejams: URL: http://www.plasmacentre.ru/file/nashy-public/75.pdf. (in Russian)

23. Ryabcev, I.A., Senchenkov, I.K. Teoriya i praktika naplavochnyh rabot. Kiev: "Ekotehnologiya", 2013. 400 s. ISBN 978-966-8409-31-8.

24. Grigoryanc, A.G., Shiganov, I.N., Misyurov, A.I. *Tehnologicheskie processy lazernoj obrabotki*. Moskva: Izdatelstvo MGTU im. N. E. Baumana, 2006. 664c. ISBN: 5-7038-2701-9. (in Russian)

25. Mahamood, R. M., Titilayo, A. E. *Functionally Graded Materials*. New York: Springer Berlin Heidelberg, 2017. 103 p. eISBN 978-3-319-53756-6.

26. Adaskin, A.M. *Instrumentalnye materialy v mashinostroenii*. Moskva: Forum, Moskva: INFRA-M, 2017. 319 s. ISBN 978-5-00-091073-3. (in Russian)

27. Breslavskij, D.V. *Marochnik stali i splavov*. [online]. Harkov, 2003. Data dostupa: 5 aprelya 2018. Rezhim dostupa: http://www.splav-kharkov.com/main.php/(in Russian)

28. Arhipova, I., Bāliņa, S. *Statistika ekonomikā un biznesā: risinājumi ar SPSS un MS Excel*. 2. izd. Rīga: Datorzinību centrs, 2006. 362 lpp. ISBN 9789984665191.

29. Počs, R. *Kvantitatīvās metodes ekonomikā un vadīšanā*. Mācību līdzeklis. Rīga, RTU Izdevniecība, 2003. 148 lpp.

30. Baraz, V.R., Pegashkin, V.F. *Ispolzovanie MS Excel dlya analiza statisticheskih dannyh*. 2-e izd. Nizhnij Tagil: NTI (filial) UrFU, 2014. 181 s. (in Russian)

31. Fyorster, E., Ryonc, B. *Metody korrelyacionnogo i regressionnogo analiza*. Rukovodstvo dlya ekonomistov. Moskva: Finansy i statistika, 1983. 304 s. (in Russian)

32. Grīnglazs, L., Kopitovs, J. *Matemātiskā statistika: Ar datoru lietojuma paraugiem uzdevumu risināšanai*. Rīga: Rīgas Starptautiskā ekonomikas un biznesa administrācijas augstskola, 2003. 310 lpp. ISBN 9984705064.

33. Kononyuk, A.E. *Obshaya teoriya ponyatij*. Kn. 2. Teoriya obrazovaniya ponyatij. Kiiv: "Osvita Ukrayini", 2014. 512 s. ISBN 978-966-7599-50-8. (in Russian)

34. Ishhanyan, M.V. *Matematicheskoe modelirovanie*: Uchebnoe posobie. – M.: MGUPS (MIIT), 2015. 150 s. (in Russian)

35. Karna, S. K., Sahai, R. An Overview on Taguchi Method. International Journal of Engineering and Mathematical Sciences, 2012, vol. 1, no. 1, pp. 1–7. ISSN 2319-4545.

36. Steen, W.M., Mazumder, J. *Laser Material Processing*. 4th ed., London: Springer, 2010, 558 p. ISBN 978-1-84996-061-8

37. Matsunawa, A., Kim, J.D., Seto, N., Mizutani, M., Katayama, S. *Dynamics of Keyhole and Molten Pool in Laser Welding. Journal of Laser Applications*, vol. 10, no. 6, pp. 247–254. eISSN 1938-1387. Available from: doi:10.2351/1.521858.

38. Zhou, J., Tsai, H.L. Porosity Formation and Prevention in Pulsed Laser Welding. *Journal of Heat Transfer*, 2007, vol. 129, no.8, pp. 1014–1024. *ISSN* 0022-1481. Available from: doi:10.1115/1.2724846.

39. Devoyno, O.G., Drozdov, P.S., Dovoretskiy, Y.B., Kardapolova, M.A., Lutsko, N.I., Tamanis, E. Influence of Laser Cladding Parameters on the Distribution of Elements in the Beads of Nickel-based Ni-Cr-B-Si Alloy. *Latvian Journal of Physics and Technical Sciences*, 2012, vol.49, no.4, pp. 61–70. ISSN 0868-8257. Available from: doi: 10.2478/v10047-012-0023-3.

40. Shevelkov, V.V. Tvyordost – kriterij uprochneniya metallicheskih materialov. Vestnik Pskovskogo gosudarstvennogo universiteta. Seriya: Ekonomicheskie i tehnicheskie nauki. 2014, № 5, c. 125–134. ISSN 2227-5215. Pieejams: URL: https://pskgu.ru/projects/pgu/ storage/wt/wet05/wet05_13.pdf. (in Russian)

41. Stoev, P.I., Moshenok, V.I. Opredelenie mehanicheskih svojstvmetallov i splavov po tverdosti. Vestnik Harkovskogo nauchnogo universiteta im. Karazina, 2003, t. 601, № 2(22), s. 106–112. Pieejams: URL: http://nuclear.univer.kharkov.ua/lib/601_2(22)_ 03_p106-112.pdf. (in Russian)

42. Bojko, N.I. Resursosberegayushie tehnologii povysheniya kachestva poverhnostnyh sloev detalej mashin: Uchebnoe posobie dlya vuzov zh.-d. transporta. M.: Marshrut, 2006. 198 s. ISBN 5-89035-435-3. (in Russian)

43. Klimenko, S.A., Kopejkina, M.Yu., Lavrinenko, V.I., Majboroda, V.S., Akulovich, L.M., Levin, M.L., Hejfec, M.L., Hudolej, A.L., Chizhik, S.A. Finishnaya obrabotka poverhnostej pri proizvodstve detalej. Minsk : Belaruskaya navuka, 2017. 376 s. ISBN 978-985-08-2201-7. (in Russian)

44. Pravednikov, I.S. Opredelenie napryazhenij v plasticheski deformiruemyh detalyah. *Elektronnyj nauchnyj zhurnal "Neftegazovoe delo"*, 2005, № 1, c. 38(8). eISSN 1813-503X. (in Russian)